TRANSPORT INDUCED BY ENERGETIC PARTICLE DRIVEN GEODESIC ACOUSTIC MODES

D. ZARZOSO[1], D. DEL-CASTILLO-NEGRETE[2], D. F. ESCANDE[1], Y. SARAZIN[3], X. GARBET[3], V. GRANDGIRARD[3], C. PASSERON[3], G. LATU[3], S. BENKADDA[1,5], M. SASAKI[4,5]
[1] Aix-Marseille Université, CNRS, PIIM, UMR 7345 Marseille, France.
[2] Oak Ridge National Laboratory, Oak Ridge, TN 37831-8071, United States of America
[3] CEA, IRFM, 13108 Saint-Paul-lez-Durance, France
[4] Research Institute for Applied Mechanics, Kyushu University, Kasuga 816-8580, Japan
[5] LIA-CNRS France-Japan ITER Physics Laboratory

Email of corresponding author: david.zarzoso-fernandez@univ-amu.fr

Abstract

Full-f global gyro-kinetic simulations with the GYSELA code are used to demonstrate that energetic-particle-driven geodesic acoustic modes (EGAMs) can be responsible for particle transport. This is done by coupling GYSELA to a particle tracking post-treatment code that solves the gyro-center equations of motion using the modern gyro-kinetic approach. It is shown that, even if EGAMs are axisymmetric modes, they can lead to transport of mainly counter-passing particles by conservation of the toroidal canonical momentum. The fundamental physics of the interaction between the electrostatic EGAM island and the region of magnetically trapped particles is detailed, showing a complex interplay between the electrostatic and magnetic structures that results in losses of counter-passing modulated at the EGAM frequency. The co-injection of energetic particles is therefore a possible way to minimize the losses due to EGAMs.

1. INTRODUCTION

Energetic particles (EP) exist in tokamaks due to either nuclear fusion reactions or external heating. They are characterized by supra-thermal energies and a significant fraction of EP can trigger instabilities called energetic particle modes (EPM) due to anisotropies in phase-space, which can be deleterious to the EP confinement. However, EP must be sufficiently well confined to transfer their energy to the thermal population by means of Coulomb collisions. In addition, unconfined energetic particles are dangerous because they can damage the wall components of the tokamak. Therefore, EPM and EP transport must absolutely be understood, controlled and eventually avoided. In this work, we focus on a class of EPMs called energetic geodesic acoustic modes (EGAMs) [1]. They are characterized by an axisymmetric structure and are excited by EP from the standard branch of GAMs or from an initially Landau damped mode, as was reported in [2,3]. EGAMs have been observed in many experimental devices, such JET [4,5], DIII-D [6,7] and HL-2A [8]. Their linear and nonlinear behaviors have also been modelled in gyro-kinetic [2,9,10] and hybrid [11,12] numerical simulations. Moreover, their interaction with turbulence has also been evidenced [13-15] and they have been explained in a wide variety of analytic works [16-21], including a fluid framework [22,23]. Since they are axisymmetric modes, they conserve the toroidal canonical momentum. If the toroidal velocity of gyro-centers is low enough, the momentum is approximated by the poloidal flux, which is related to the radial position of gyro-centers. Owing to the conservation of the toroidal momentum, EGAMs have therefore been believed to play little role on the transport of particles. However, one should consider the information of both the radial position and the toroidal velocity of gyro-centers when using the conservation of the toroidal canonical momentum. When doing this, one can show that a modification in the toroidal velocity of particles can potentially lead to a modification in their radial position. Therefore, EGAMs might play a similar role to collisions, modifying the pitch-angle of particles. This was conjectured in [6], after observing in DIII-D discharges that the activity of EGAMs is correlated to drops in the neutron emission, which is indicative of energetic particle losses. Later, a Fast Ion Loss Detector (FILD) [24] was installed on DIII-D to diagnose the losses of EP in the presence of EGAMs. Dedicated experiments on DIII-D [7] corroborated that EGAM activity is correlated to the losses of EP measured by the FILD diagnostic. Also, the losses were found to be dominated by the EGAM frequency. The characteristics of lost particles given by the FILD diagnostic were later used in the full-orbit SPIRAL code [25] to follow the lost particles back to the moment when they were confined. These numerical simulations found that indeed counter-passing particles are trapped and subsequently lost. Finally, very recent gyro-kinetic simulations provided more details on the fundamental mechanism for this transport [26]. The remainder of the paper is structured as follows. In section 2, we give a brief explanation of GYSELA and the simulations run to obtain the electrostatic potential. In section 3, we describe the code that has been developed to analyze the transport of gyro-centers and show the evidences of gyro-center transport in the presence of EGAMs. Finally, conclusions and forthcoming work are presented in section 4.

2. EGAMS IN GYSELA

The linear excitation of EGAMs is analyzed starting from the Vlasov equation

$$\frac{\partial F}{\partial t} - [H, F] = 0$$

with F the total distribution function, H the Hamiltonian and $[H, F]$ represents the Poisson bracket between the Hamiltonian and the distribution function, which can be written in terms of action-angle variables as

$$[H, F] = \frac{\partial H}{\partial \boldsymbol{\alpha}} \cdot \frac{\partial F}{\partial \boldsymbol{J}} - \frac{\partial H}{\partial \boldsymbol{J}} \frac{\partial F}{\partial \boldsymbol{\alpha}}$$

where $\boldsymbol{\alpha}$ is the vector containing the three angles characterizing the periodic motion of particles in the tokamak and $\boldsymbol{J}$ is the vector containing the three actions, which are the motion invariants in the presence of an equilibrium Hamiltonian, i.e. when the Hamiltonian does not depend on the angles. The distribution function and Hamiltonian can be decomposed into equilibrium and perturbed components

$$F = F_{eq} + \delta F, H = H_{eq} + \delta H$$

Injecting these decompotions into the Vlasov equation, projecting onto a Fourier basis and linearising gives the perturbed distribution function

$$\delta F = -\sum_{\boldsymbol{n},\omega} \frac{\boldsymbol{n} \cdot \partial_J F_{eq}}{\omega - \boldsymbol{n} \cdot \boldsymbol{\Omega}} \delta H_{\boldsymbol{n}\omega} e^{i(\boldsymbol{n}\cdot\boldsymbol{\alpha} - \omega t)}$$

with ω the frequency of the mode, $\boldsymbol{n} = (n_1, n_2, n_3)$ the wave number, $\boldsymbol{\Omega} = (\Omega_1, \Omega_2, \Omega_3)$ the eigenfrequencies of the system and $\delta H_{\boldsymbol{n}\omega}$ the $(\boldsymbol{n}, \omega)$ Fourier mode of the perturbed Hamiltonian. The system can be closed by means of the quasi-neutrality equation

$$n_e = \sum_s Z_s n_s$$

with n_s the density of ion species s, Z_s the charge number of species s and n_e the electron density. In the followoing we will use the gyro-kinetic approach, in which the plasma response is averaged over the fast cyclotron motion. Mathematically, this means that $n_1 = 0$. If we take into account only deeply passing ions, it can be shown that the resonant condition (the denominator of the perturbed distribution function) is written as $\omega - m\frac{v_{||}}{qR_0} = 0$, where m is the poloidal mode number, R_0 is the major radius measured at the magnetic axis, q is the safety factor and $v_{||}$ is the component of the velocity parallel to the magnetic field lines. The density is calculated by integration in velocity space, which, after being introduced in the quasi-neutrality condition, will give the dispersion relation for the mode. It is to be noted that the numerator, for axisymmetric modes (the case of EGAMs), reduces to $\omega\partial_E F_{eq}$, which intuitively shows that if there is a positive slope of the distribution function around the resonant velocity the mode can be excited. This dispersion relation was solved in [2,3] and compared to gyro-kinetic simulations in [2] for one energetic particle species and in [26] for a scan on the charge and mass number of energetic particles to analyse the isotope dependence on the EGAM excitation. In the present work we focus our analysis on GYSELA simulations. GYSELA [27] is a full-*f* global flux-driven gyro-kinetic code, which was initially developed for the analysis of electrostatic turbulence in tokamaks. In the past years, GYSELA have been updated to include new physics. One of these updates includes the presence of EP. There are typically two ways to introduce EP in the code. The first method is introducing the energetic particles as an initial equilibrium distribution function, as done analytically earlier in this section. If the distribution function depends only on the motion invariants, it does not evolve in time unless instabilities are triggered. This method is useful to verify the code against linear analytic calculations. The second method is introducing energetic particles by means of a source that builds the distribution function. This method was used in [13-15] for the analysis of the interaction between energetic particles and turbulence via the excitation of EGAMs and is required in the presence of gradients because the distribution function has to be maintained. In this work we will perform GYSELA simulations using the first method of introducing energetic particles. Electrons will be assumed adiabatic in the

remainder of the paper and two kinetic ion species are employed: thermal ions modelled by a centered Maxwellian and energetic ions modelled by a double-shifted Maxwellian as in [2]. The idea of introducing a symmetric distribution function for energetic ions is to avoid the introduction of any moment that might modify the excitation of EGAMs. The thermal and energetic particle densities satisfy the quasi-neutrality condition. In addition, the fact that we use separate species for thermal and energetic ions allows one to determine to what extent the excitation of EGAMs by energetic particles affects the thermal population. In particular, the existence of higher order resonances can lead to significant interaction between the energetic and thermal particles through the excitation and damping of EGAMs. The linear excitation of the EGAM and nonlinear saturation using the multi-species version of GYSELA were analyzed in detail in [26]. Here we give just a brief description of the main results. For this purpose, 2% of the total ion population will be composed of energetic ions with a mean velocity $v_0 = 6v_{th}$. The width of their associated shifted Maxwellian is $T_{EP} = 2T_{th}$, with T_{th} the temperature of thermal ions. This population results into a positive growth rate $\gamma \approx 1.7 \cdot 10^{-4}\omega_{c0}$, with ω_{c0} the cyclotron frequency of thermal ions, and a frequency $\omega \approx 3.8 \cdot 10^{-3}\omega_{c0}$, which are the same as the ones provided by the analytic theory [3]. The time trace of the electrostatic potential is shown in the left panel of FIG. 1, where the linear excitation phase is clearly observed. After this linear phase, a nonlinear saturation leads to the modification of the distribution function, as explained earlier in this section. This modification can be seen in the right panel of FIG. 1 for both energetic (red dashed line) and thermal (blue solid line) ions, with a structure that leads to the flattening of the distribution function, as observed in [9]. The modification of the distribution function occurs around the resonant positions between particles and the mode. This positions are identified by the poloidal harmonics *m=1* (the main resonance around the velocity $v_{||}$=*4.5*v_{th}) and m=2 (around $v_{||}$=*2.25*v_{th}).

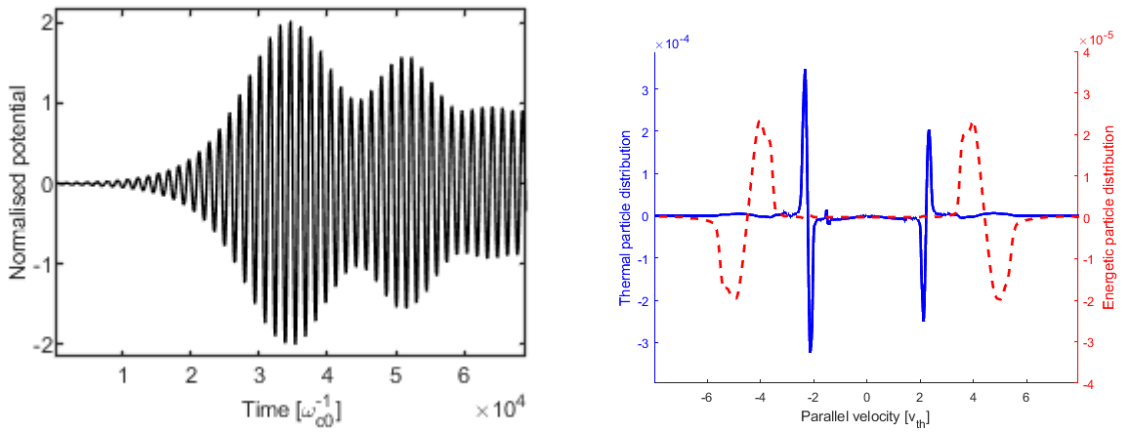

FIG. 1. (Left) Time trace of the electrostatic potential with 2% energetic ion fraction. (Right) Perturbed distribution function for energetic (dashed line) and thermal (solid line) ions, as a function of the parallel velocity normalised to the thermal velocity

The right panel of FIG. 1 shows the dependence of the perturbed distribution function on the parallel velocity. However, this has been obtained by averaging the distribution over the poloidal angle. Without averaging, the distribution function shows an island structure in the sub-space of parallel velocity and poloidal angle. This is clearly observed in FIG. 2 for thermal (left panel) and energetic (right panel) ions. This figure has been produced to highlight the formation of the island around the resonant positions in parallel velocity and therefore do not cover the whole velocity interval of the simulations. Note in particular that for thermal particles there is an island satisfying *m=2*. Particles that are close to the resonance will tend to synchronize with the mode and can be nonlinearly trapped inside the island. This induces periodic oscillations of their parallel velocity and therefore, by conservation of the toroidal canonical momentum, periodic oscillations of their radial positions.

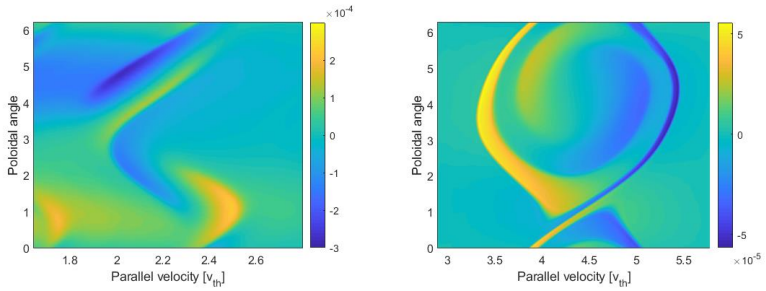

FIG. 2. Detail of the perturbed distribution function around the resonances m=2 (left) and m=1 (right) as a function of the poloidal angle and the parallel velocity for thermal (left) and energetic (right) ions.

It is to be noted that the EGAM islands shown in FIG. 2 exhibit an electrostatic nature and therefore the trapping of particles inside those islands is purely electrostatic. However, we have shown here that there are several poloidal harmonics associated with the EGAM. For a given frequency, the higher the poloidal harmonic, the smaller the resonant velocity around which the island forms. And for a given magnetic moment, the smaller the parallel velocity, the closer the particle gets to the magnetically trapping domain, which we will call trapping cone in the following. If the EGAM islands are sufficiently close to the trapping cone, one might expect that at some point the particles can be magnetically trapped and if their banana orbits are wide enough they can be lost as conjectured in [6] and later demonstrated in [7]. In the next section we will show that this transport in phase space, from the moment when particles are electrostatically trapped inside the EGAM to the moment when they are magnetically trapped and lost, is due to a chaotic regime originated by the interaction between the EGAM and the trapping cone.

3. PASSIVE GYRO-CENTERS TRACKING AND EGAM LOSSES

In order to analyze and characterize the transport of particles in the presence of EGAMs, we use the electrostatic potential obtained from the GYSELA simulations with 2% energetic ion fraction and inject it into a recently developed code that solves the equations of motion for test gyro-centers within the modern gyro-kinetic approach. For the sake of simplicity, we do not provide here the set of equations to be solved. The interested reader can find them as well as the method used to integrate them in [26]. The test gyro-centers are initialized at the same poloidal and toroidal angles. Half of the particles are initialized at the 20% of the minor radius and the other half at the 60% of the minor radius. The set of test gyro-centers is initialized uniformly in parallel velocity and magnetic moment. The particles are tracked until they eventually reach the boundary domain and a label *lost* is associated to those particles. Then, the lost particles are indicated in a diagram as a function of their initial parallel velocity and magnetic moment and their initial radial position. This is shown in FIG. 3 (left: particles initialized at 20% of the minor radius, right: particles initialized at 60% of the minor radius), where the solid line represents the separation between magnetically passing (outside the line) and magnetically trapped (inside the line) particles. The grey area represents particles that are never lost and the black area represents particles that are lost even in the absence of EGAMs. These losses are called *prompt losses* and correspond to particles that are initialized in such a way that their orbits intercept the boundary from the very beginning of the simulation. The white area represents particles that are lost only in the presence of EGAMs. These losses will therefore be called *EGAM losses*. It can be observed that the EGAM losses occur for counter-passing particles, as reported in [7].

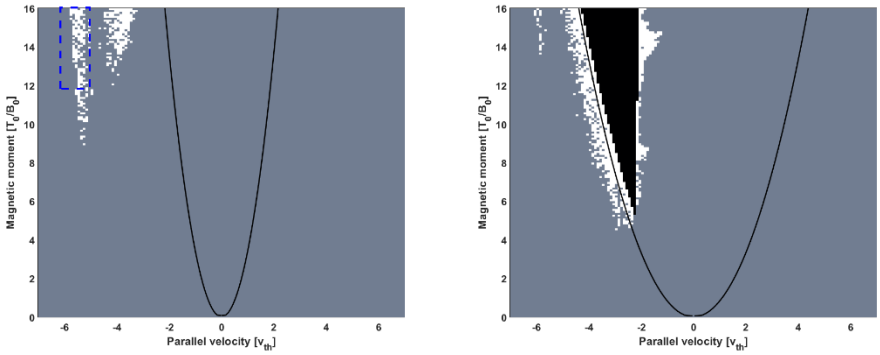

FIG. 3. Losses of particles initiliazed at 20% (left) and 60% (right) of the minor radius. Black regions indicate prompt losses. White regions indicate EGAM losses. The solid line represents the trapping cone.

In the left panel of FIG. 3 it becomes evident that the EGAM losses are arranged following two bands. These bands are located around the resonant velocities at *m=1* and *m=2*. Therefore, the EGAM losses can be considered as resonant losses. In the right panel, the band corresponding to the resonant velocity at *m=2* is already inside or too close to the trapping domain. In order to shed more light on the mechanism for the transport and losses of energetic ions, we analyze and classify further the EGAM losses by performing a simulation of test gyro-centers initialized inside the dashed blue rectangle shown in the left panel of FIG. 3. An example of one of these particles in shown in the left panel of FIG. 4, where the projection onto the poloidal cross-section of its trajectory is plotted. The time trace of its parallel velocity is given in the right panel of the same figure by the blue line. It can be seen that this particle is initially counter-passing and, as it synchronizes with *m=1* and afterwards with *m=2* poloidal harmonics of the EGAM (given by the horizontal dashed lines) it gets closer to the magnetically trapping cone, which results in the trapping of the particle and eventual loss. The right panel of FIG. 4 also gives the time trace of two other particles whose initial conditions are slightly different. The dynamics of these particles seems to be very disparate and whereas one particle exit very early the system, another one takes much longer to reach the boundary.

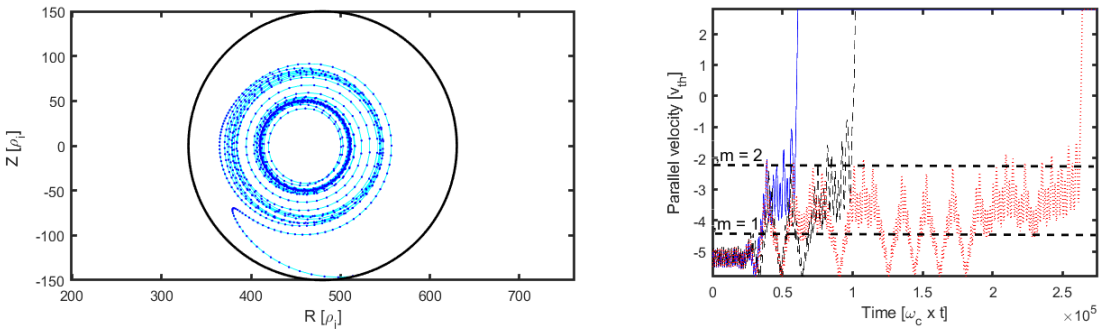

FIG. 4. (Left) Poloidal cross-section of the trajectory of one particles initialized inside the blue rectangle of FIG. 3. (Right) Time trace of the parallel velocity of three particles initialized inside the blue rectangle of FIG. 3 with very close initial conditions. The horizontal dashed lines represent the resonant velocities for the poloidal harmonics m=1 and m=2.

This behavior is characteristic of chaotic regimes. The exit time can also provide important information about the types of EGAM losses. For instance, prompt losses must be characterized by small exit times, whereas losses like the one given by the red line of FIG. 4 should be characterized by larger exit times. The inverse of the exit time is plotted in FIG. 5, normalized to the EGAM saturation time (indicated by the vertical line). Losses on the right side of the vertical line occur before the EGAM saturation and are therefore dominated by linear effects, whereas losses on the left side occur after the EGAM saturation and are therefore dominated by nonlinear effects. It is observed that the losses are clearly divided into these two groups. In addition, for the losses identified as linearly dominated, two sub categories can be made: the prompt losses which occur even before the EGAM is excited and the enhanced prompt losses, which occur when the EGAM is excited but before the nonlinear saturation. Two examples of these enhanced prompt losses are given in the right panel of FIG. 5. It is observed that these losses correspond to particles that are initially close to the trapping cone. Any perturbation of the system, for example the EGAM during its linear phase, can provide energy to those particles so that they fall into the trapping cone

and are lost. In the left panel of FIG. 5 we see that most of the losses in the inner region of the tokamak are due to nonlinear effects.

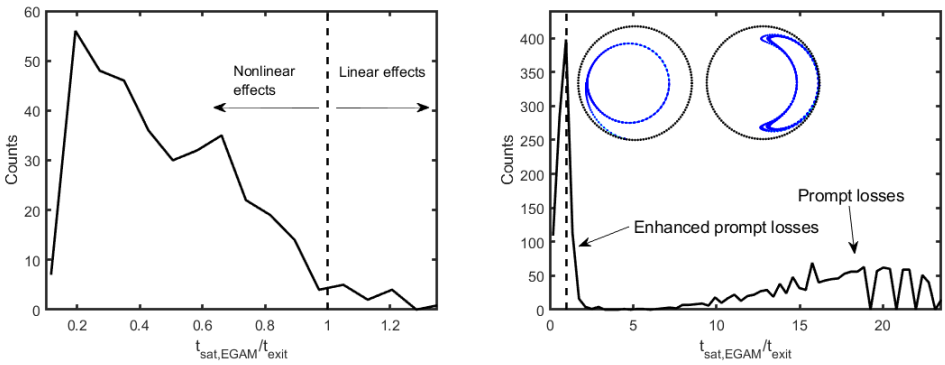

FIG. 5. Inverse of the exit time normalized to the EGAM saturation time (dashed vertical line) for particles initialized inside the blue rectangle of FIG. 3 at 20% of the minor radius (left) and 60% of the minor radius (right). In the right panel, two examples of losses identified as enhanced prompt losses during the linear phase of the EGAM.

The reason why these particles take longer times to exit the tokamak can be found in the chaotic regime of the system invoked earlier. The chaotic regime is evidenced by plotting the position of the particles in phase-space (radius, poloidal angle and parallel velocity). This is shown in FIG. 6, where the positions are projected onto the $(v_{||}, r)$ (left), (r, θ) (middle) and $(v_{||}, \theta)$ (right) sub-spaces. For the sake of simplicity, the radial position of the particles is also identified by colors (blue indicates inner radial positions and red outer radial positions). In this figure, the EGAM island is clearly visible in the middle and right panels, whereas in the left panel no island is observed. This evidences that the EGAM is a mode characterized by its poloidal structure $\sim \sin\theta$ which occurs by resonance with the parallel motion of particles, which is related to the radial position by the conservation of the toroidal canonical momentum. The left panel of FIG. 6 simply represents the surface where the toroidal momentum is constant, which is a surface that constraints the motion of particles.

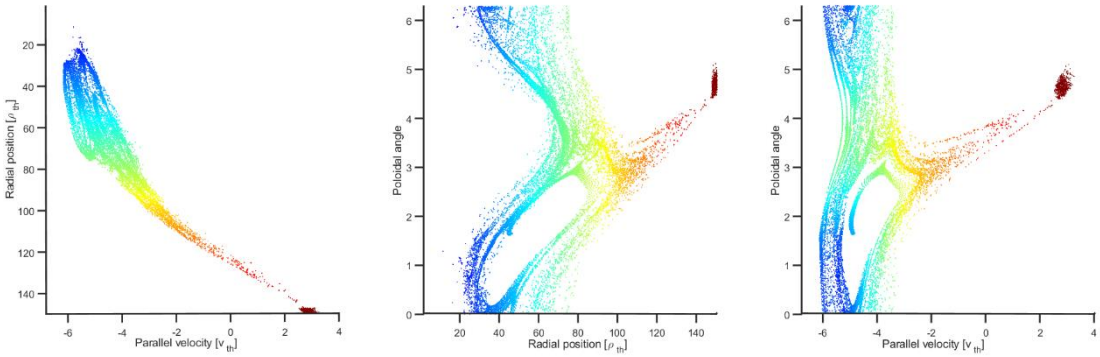

FIG. 6. Position of test gyro-centers in phase-space, projected onto different sub-spaces.

The results provided in FIG. 6 indicate that there is an interaction between the (electrostatic) EGAM island and the (magnetic) trapping cone. This is evidenced by the way particles are lost by means of a channel that goes through the X-point of the trapping cone (not shown here). More details about this phenomenon can be found in [26]. The fact that the losses occur every time the EGAM island gets closer to the X-point of the trapping cone leads to losses modulated at the EGAM frequency, as can be seen in FIG. 7, where the time trace of the losses are plotted together with their Fourier transform, indicating a dominant peak at the EGAM frequency.

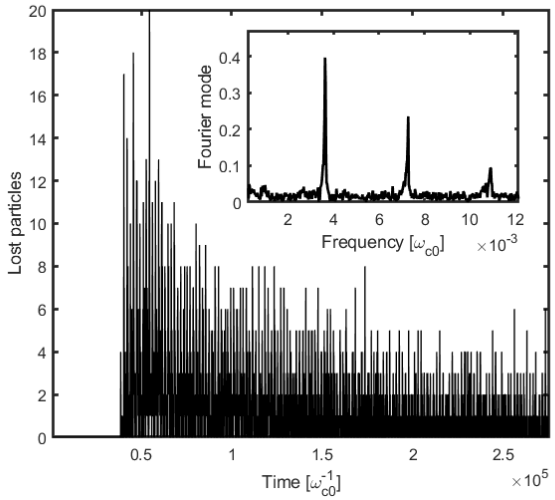

FIG. 7. Time trace of the losses of particles with their Fourier transform indicating that losses occur at the EGAM frequency.

4. CONCLUSIONS

In this work, we have analysed the transport of particles in a tokamak due to the excitation of energetic-particle-driven geodesic-acoustic-modes (EGAMs). This has been done by means of GYSELA simulations and a test gyro-center tracking code that has been developed to integrate the trajectories using the self-consistent EGAM electrostatic potential obtained from GYSELA simulations. We have shown that the flattening of the distribution function in velocity space occurs with the formation of an island in (r, θ) and $(v_{||}, \theta)$ sub-spaces, centred around the main EGAM resonant velocity. We have shown that EGAMs induce particle losses, which are classified into EGAM enhanced prompt losses (or linearly induced losses) and nonlinearly induced EGAM losses. We have also provided evidence that these losses are due to the interaction between the EGAM island and the trapping cone, creating a chaotic channel of transport from counter-passing to trapped particles that result in losses modulated at the EGAM frequency. This work opens new perspectives for further analysis to optimize the injection of energetic particles to minimize the losses due to EGAMs.

ACKNOWLEDGEMENTS

This work has been carried out thanks to the support of the A*MIDEX project (no. ANR-11-IDEX-0001-02) funded by the Investissements d'Avenir French Government program, managed by the French National research Agency (ANR). This work has also been carried out within the framework of the EUROfusion Consortium and has received funding from the Euratom research and training programme 2014–2018 under grant agreement no. 633053. The views and opinions expressed herein do not necessarily reflect those of the European Commission. D. dCN acknowledges support from the Oak Ridge National Laboratory, managed by UT-Battelle, LLC, for the U.S. Department of Energy under Contract No. DE-AC05- 00OR22725. This work was granted access to the HPC resources of TGCC under the allocation t2016057653 and to the HPC resources of CINES under the allocation A0020507653 made by GENCI (Grand Equipement National de Calcul Intensif). This work has been done within the framework of the Nonlinear energetic particle dynamics (NLED) European Enabling Research Project (EUROFUSION AWP15-ER-01/ENEA-03) and within the framework of the Verification and development of new algorithms for gyrokinetic codes European Enabling Research Project (EUROFUSION AWP15-ER-01/IPP-01).

REFERENCES

[1] FU G. 2008 *Phys. Rev. Lett.* **101** 185002
[2] ZARZOSO D. *et al* 2014 *Nucl. Fusion* **54** 103006
[3] GIRARDO J.-B., ZARZOSO D., *et al* 2014 *Phys. Plasmas* **21** 092507
[4] BOSWELL C., BERK H., *et al* 2006 *Phys. Lett.* A **358** 154–8
[5] BERK H. *et al* 2006 *Nucl. Fusion* **46** S888
[6] NAZIKIAN R. *et al* 2008 *Phys. Rev. Lett.* **101** 185001
[7] FISHER R., *et al* 2012 *Nucl. Fusion* **52** 123015
[8] CHEN, W., *et al.* 2013 *Nuclear Fusion* **53** 113010

[9] ZARZOSO D. *et al* 2012 *Phys. Plasmas* **19** 022102
[10] BIANCALANI A *et al* 2014 *Nucl. Fusion* **54** 104004
[11] WANG H. *et al* 2013 *Phys. Rev. Lett.* **110** 155006
[12] WANG H. *et al* 2015 *Phys. Plasmas* **22** 092507
[13] ZARZOSO D. *et al* 2013 *Phys. Rev. Lett.* **110** 125002
[14] DUMONT R. *et al* 2013 *Plasma Phys. Control. Fusion* **55** 124012
[15] ZARZOSO D. *et al* 2017 *Nucl. Fusion* **57** 072011
[16] BERK H. AND ZHOU T. 2010 *Nucl. Fusion* **50** 035007
[17] QIU Z., ZONCA F. AND CHEN L. 2010 *Plasma Phys. Control. Fusion* **52** 095003
[18] SASAKI M., ITOH K. AND ITOH S. 2011 *Plasma Phys. Control. Fusion* **53** 085017
[19] REN H. AND DONG C. 2014 *Phys. Plasmas* **21** 102506
[20] SASAKI M., *et al* 2016 *Phys. Plasmas* **23** 102501
[21] REN H. 2016 *Nucl. Fusion* **57** 016023
[22] QU Z., HOLE M. AND FITZGERALD M. 2016 *Phys. Rev. Lett.* **116** 095004
[23] QU Z., HOLE M. AND FITZGERALD M. 2017 *Plasma Phys. Control. Fusion* **59** 055018
[24] GARCIA-MUNOZ M., *et al* 2009 *Rev. Sci. Instrum.* **80** 053503
[25] KRAMER G., *et al* M. 2013 *Plasma Phys. Control. Fusion* **55** 025013
[26] ZARZOSO, D., DEL-CASTILLO-NEGRETE, D., ESCANDE, D. F., *et al.* 2018 *Nuclear Fusion* **58** 106030
[27] GRANDGIRARD V. *et al* 2016 *Comput. Phys. Commun.* **207** 35–68